International Journal of Biomedical Materials Research
2015; 3(6): 83-91
Published online December 21, 2015 (http://www.sciencepublishinggroup.com/j/ijbmr)
doi: 10.11648/j.ijbmr.20150306.12
ISSN: 2330-7560 (Print); ISSN: 2330-7579 (Online)

Characterization of Physicochemical and Thermal Properties of Biofield Treated Ethyl Cellulose and Methyl Cellulose

Mahendra Kumar Trivedi[1], Alice Branton[1], Dahryn Trivedi[1], Gopal Nayak[1], Rakesh Kumar Mishra[2], Snehasis Jana[2, *]

[1]Trivedi Global Inc., Henderson, USA
[2]Trivedi Science Research Laboratory Pvt. Ltd., Bhopal, Madhya Pradesh, India

Email address:
publication@trivedisrl.com (S. Jana)

To cite this article:
Mahendra Kumar Trivedi, Alice Branton, Dahryn Trivedi, Gopal Nayak, Rakesh Kumar Mishra, Snehasis Jana. Characterization of Physicochemical and Thermal Properties of Biofield Treated Ethyl Cellulose and Methyl Cellulose. *International Journal of Biomedical Materials Research.* Vol. 3, No. 6, 2015, pp. 83-91. doi: 10.11648/j.ijbmr.20150306.12

Abstract: Cellulose and its derivatives are used as potential matrices for biomaterials and tissue engineering applications. The objective of present research was to investigate the influence of biofield treatment on physical, chemical and thermal properties of ethyl cellulose (EC) and methyl cellulose (MC). The study was performed in two groups (control and treated). The control group remained as untreated, and biofield treatment was given to treated group. The biofield treated polymers are characterized by Fourier transform infrared spectroscopy (FT-IR), CHNSO analysis, X-ray diffraction study (XRD), Differential Scanning calorimetry (DSC), and thermogravimetric analysis (TGA). FT-IR analysis of treated EC showed downward shifting in C-O-C stretching peak from 1091→1066 cm^{-1} with respect to control. However, the treated MC showed upward shifting of –OH stretching (3413→3475) and downward shifting in C-O stretching (1647→1635 cm^{-1}) vibrations with respect to control MC. CHNSO analysis showed substantial increase in percent hydrogen and oxygen in treated polymers with respect to control. XRD diffractogram of EC and MC affirmed the typical semi-crystalline nature. The crystallite size was substantially increased by 20.54% in treated EC with respect to control. However, the treated MC showed decrease in crystallite by 61.59% with respect to control. DSC analysis of treated EC showed minimal changes in crystallization temperature with respect to control sample. However, the treated and control MC did not show any crystallization temperature in the samples. TGA analysis of treated EC showed increase in thermal stability with respect to control. However, the TGA thermogram of treated MC showed reduction in thermal stability as compared to control. Overall, the result showed substantial alteration in physical, chemical and thermal properties of treated EC and MC.

Keywords: Biofield Treatment, Ethyl Cellulose, Methyl Cellulose, X-ray Diffraction Study, Differential Scanning Calorimetry, Thermogravimetric Analysis, Fourier Transform Infrared Spectroscopy

1. Introduction

Tissue engineering is an interdisciplinary area that uses cells, materials, engineering and life sciences toward the design and fabrication of biological substitutes that restore, support, or improve tissue or a whole organ function. Biomedical implant scaffolds are an excellent example of tissue engineering substrates composed of biodegradable polymers or inert materials coated with bioactive biomaterials which allows growth of new tissues of particular types of cells [1, 2]. Biomaterials need to be properly modified by introducing controlled porosity, design of three-dimensional structure and surface modification to achieve better cell packing and control cell network architecture [3-8]. The biomaterial scaffold should have biodegradable and biocompatible nature. After the formation of the new tissue, polymeric scaffolds are slowly degraded into small molecular weight compounds, which was absorbed by the body or excreted out of the body [9].

In last few years hunt for new classes of biomaterials, with specific properties to be used as scaffolds for tissue engineering, has attained great interest, like cellulose, polyhydroxyalkanoates, polylactates and blends of these

polymers [10-15]. Recently few cellulose polymers have demonstrated excellent three-dimensional structure, water retention, high mechanical strength and biocompatibility which enable their usefulness for skin tissue regeneration [16, 17]. For example, one of the cellulose derivative bacterial cellulose has shown great potential due to its biocompatible and hygienic nature perfectly cater to the specific demand of wound tissue repair. Methyl cellulose (MC) being a derivative of cellulose family is one of the popular polymer where the –OH group are replaced by methoxyl group [18]. MC was used to prepare hydrogels by crosslinking with dialdehyde in presence of a strong acid. MC is biodegradable in nature, and popular for many biomedical applications such as drug delivery [19] and wound healing [20]. On the other hand EC is a hydrophobic polymer used as sustained release carrier; and commonly used in drug and biomedical industries for its high biodegradability and biocompatibility [21]. However, hydrophobic nature of EC and low mechanical strength of MC matrices lowers its applicability as biomaterials and tissue engineering applications. Therefore in the present work an attempt has been made to modify the properties of these cellulosic polymers (EC and MC) by biofield treatment.

It is already established that electrical currents coexist along with the magnetic field inside the human body [22]. Mr. Trivedi has the ability to harness the energy from environment or universe and can transmit into any object (living or nonliving) around this Globe. The biofield treatment has significantly enhanced the atomic and thermal properties of metals [23-26]. Additionally, the biofield treatment is known to alter the characteristics of many things in other research fields also such as, microbiology [27-29], agriculture [30-33] and biotechnology [34].

By considering above mentioned excellent results outcome from biofield treatment an attempt has been made in this work to study the physical, chemical and thermal properties of EC and MC.

2. Materials and Methods

Ethyl cellulose and Methyl cellulose were procured from Sigma Aldrich, USA. The sample was divided into two parts; one was kept as a control sample, while the other was subjected to Mr. Trivedi's biofield treatment and coded as treated sample. The treatment group was in sealed pack and handed over to Mr. Trivedi for biofield treatment under laboratory condition. Mr. Trivedi provided the treatment through his energy transmission process to the treated group without touching the sample. The control and treated samples of EC and MC were characterized by FT-IR, CHNSO, XRD, DSC and TGA.

2.1. Fourier Transform Infrared (FT-IR) Spectroscopy

The infrared spectra of control and treated EC and MC were recorded with Fourier Transform Infrared (FT-IR) Spectrometer, Perkin Elmer, USA. FT-IR spectrum was recorded in the range of 500-4000 cm^{-1}.

2.2. CHNSO Analysis

The control and treated EC and MC were analysed for their elemental composition (C, H, N, O, S etc.). The powdered polymer samples were subjected to CHNSO Analyser using Model Flash EA 1112 Series, Thermo Finnigan Italy.

2.3. X-ray Diffraction (XRD) Study

XRD of control and treated EC and MC were analysed by using Phillips Holland PW 1710 X-ray diffractometer system. The wavelength of the radiation was 1.54056 angstrom. The data was obtained in the form of 2θ versus intensity (a.u) chart. The obtained data was used for calculation of crystallite size using the following formula.

$$\text{Crystallite size} = k\lambda / b \cos\theta \quad (1)$$

Where λ is the wavelength, k is the equipment constant (0.94) and b is full width half maximum (FWHM) of peaks.

2.4. Differential Scanning Calorimetry (DSC) Study

The control and treated polymers (EC and MC) were used for DSC study. The samples were analysed by using a Pyris-6 Perkin Elmer DSC on a heating rate of 10°C /min under air atmosphere.

2.5. Thermogravimetric Analysis (TGA)

Thermal stability of the control and treated EC and MC were analysed by using Metller Toledo simultaneous thermogravimetric analyser and differential thermal analysis (DTA). The samples were heated from room temperature to 400°C with a heating rate of 5°C/min under air atmosphere.

3. Result and Discussions

3.1. FT-IR Spectroscopy

FT-IR spectroscopy was used to evaluate the influence of biofield treatment on chemical nature of EC and MC (Fig. 1). FT-IR of EC showed characteristic peaks at 2974 cm^{-1} and 2869 cm^{-1} due to C–H stretching vibration peak. The –OH stretching vibration peak was observed at 3485 cm^{-1} in the control EC. The other important peaks at 1091, and 1373 cm^{-1} corresponded to C-O–C stretching and C–H bending respectively [35]. The FT-IR spectrum of treated EC sample showed important peaks for –CH stretching at 2873, 2976 cm^{-1} and –OH stretching peak was evidenced at 3485 cm^{-1}. Vibration peaks at 1066 and 1375 cm^{-1} were mainly due to C-O–C stretch and C–H bending, respectively. The result showed that C-O-C stretch present in control EC at 1091 cm^{-1} was shifted downward to 1066 cm^{-1} in treated EC. Hence, it is assumed that biofield treatment may reduce the bond strength and force constant of C-O-C bond with respect to control.

FT-IR spectrum of MC showed a typical peak at –OH stretching vibration peak at 3413 cm^{-1} [36] and C–H stretching vibration peaks at 2902 and 2835 cm^{-1} [37]. C–O

carbonyl stretching peak was observed at 1647 cm^{-1} and ring stretching was observed at 948 cm^{-1} (Fig. 2). Additionally, the peak at 1373 cm^{-1} corresponded to MC C–H bending. However, the FT-IR of biofield treated MC sample showed a downstream shifting of C-O group stretching (12 cm^{-1}) peak at 1647→1635 cm^{-1} in the sample. Moreover, an upward shifting in –OH group stretching 3413→3475 cm^{-1} was observed in treated MC. The strength of bond considerably affected the energy of the covalent bonds on interactive species. Hence, it is presumed that biofield treatment may induce changes in bond strength and force constant of the treated MC with respect to control.

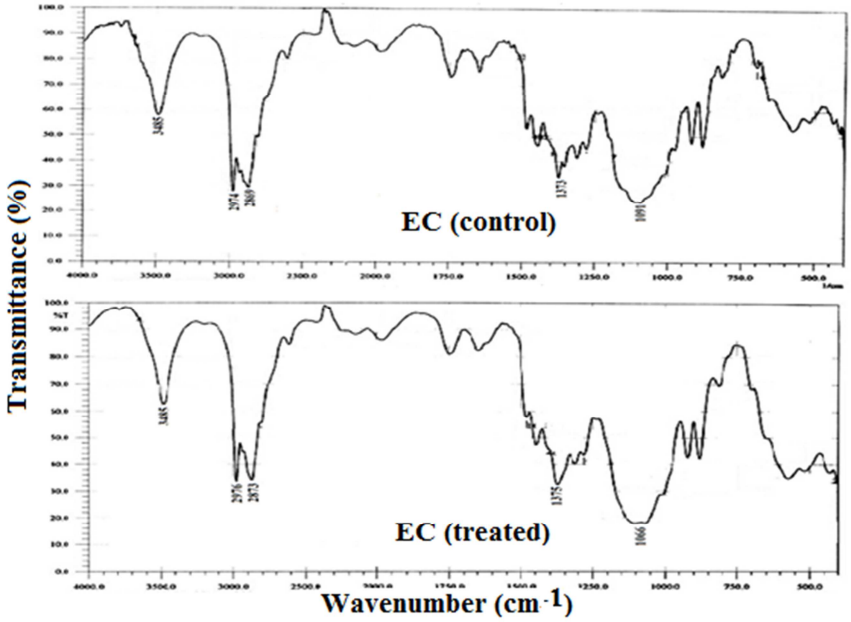

Fig. 1. *FT-IR spectra of control and treated Ethyl cellulose.*

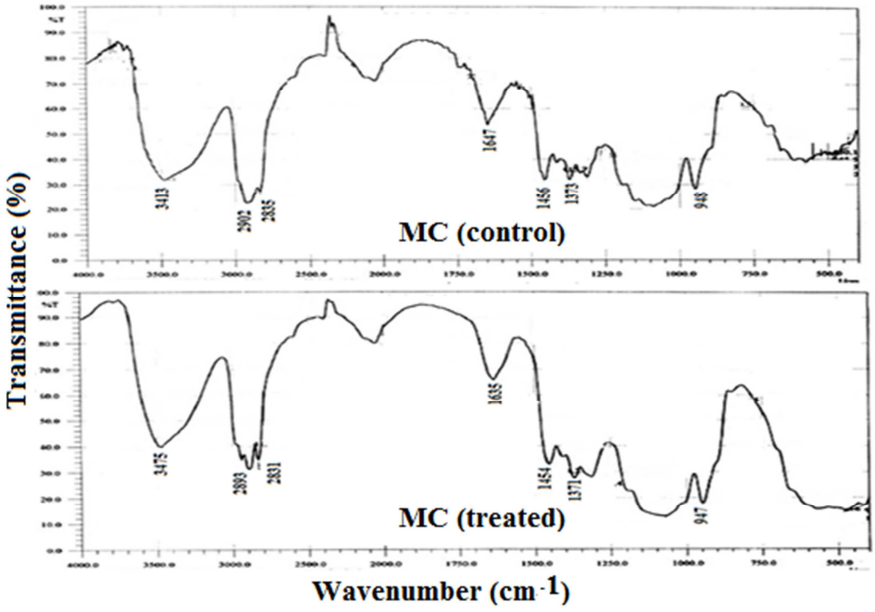

Fig. 2. *FT-IR spectra of control and treated methyl cellulose.*

3.2. CHNSO Analysis

CHNSO analysis was conducted on treated and control samples of EC and MC. The CHNSO results are shown in Table 1. The result showed that the treated EC has 9.41% increase in hydrogen and 14.60% increase in oxygen element as compared to control. The treated MC also showed increase in percentage hydrogen (8.08%) however, change in oxygen (1.46%) was not significant in treated MC. Additionally, treated EC showed decrease in 0.21 percentage carbon as compared to control polymer; and treated MC showed decrease by 4.13 of percentage carbon as compared to control. It suggests that biofield treatment may induce changes in elemental composition of the treated EC and MC.

Table 1. *CHNSO results of ethyl cellulose and methyl cellulose.*

Element	Parameter	Ethyl cellulose	Methyl cellulose
C	Control	56.06	48.28
	Treated	55.95	46.28
	% Change	-0.21	-4.13
H	Control	9.10	6.99
	Treated	9.96	7.56
	% Change	9.41	8.08
N	Control	0.00	0.00
	Treated	0.00	0.00
	% Change	-	-
O	Control	23.67	29.49
	Treated	27.13	29.92
	% Change	14.60	1.46

The elements present in polymers are presented in percentage.

3.3. X-ray Diffraction Studies

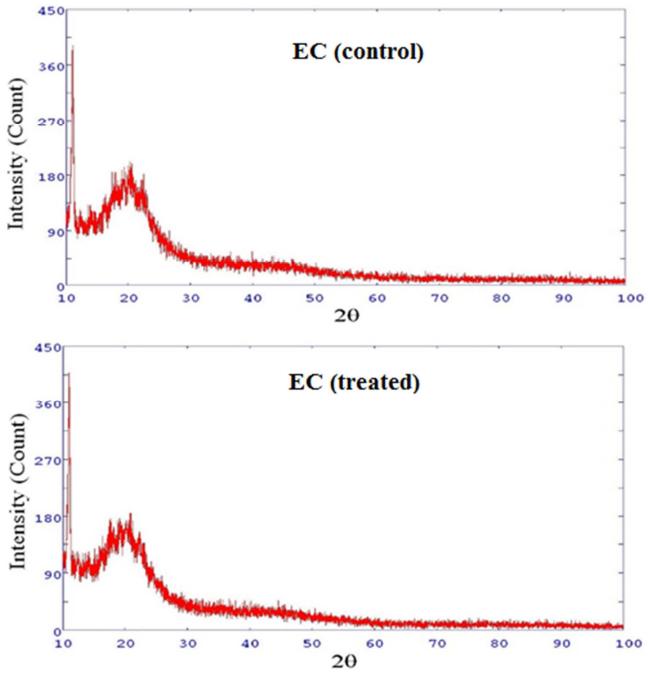

Fig. 3. *XRD diffractograms of control and treated ethyl cellulose.*

X-ray diffraction studies were conducted on control (EC and MC) and treated polymer samples. XRD diffractograms of control and treated polymer samples were illustrated in Fig. 3. XRD diffractogram of control EC showed peaks at 2θ equals to 11.05º and 20.31º. However, the XRD diffractogram of treated EC showed peaks at 2θ equals to 11.04º and 22.28º (Fig. 3). This showed no significant change in XRD pattern of treated EC with respect to control. XRD diffractograms of control and treated EC showed semi-crystalline nature of the polymer. The percentage crystallite size of the treated and control EC and MC samples were computed and reported in Fig. 4. The crystallite size of the treated EC sample was increased (10.74 nm) as compared to control sample (8.91 nm). The percentage change in crystallite size was 20.54% which showed significant change in terms of crystallite size in treated EC. It was reported previously that increase in processing temperature significantly affects the crystallite size of the materials. The increase in temperature causes decrease in dislocation density and increase in number of unit cell which ultimately causes increase in crystallite size [38, 39]. Hence, it is hypothesized that biofield treatment may provide some thermal energy to treated EC that possibly cause elevation in crystallite size of with respect to control.

X-ray diffractogram of control MC showed a broad peak at 2θ equals to 18.00º. The control MC polymer showed semi-crystalline nature with peak at 2θ equals to 20.02º (Fig. 5). This showed no change in intensity of XRD peaks of treated MC with respect to control. The control MC showed crystallite size, 83.22 nm and it was decreased to 31.96 nm in treated MC. The percentage crystallite size was decreased by -61.59%, when compared with control sample. This may be due to fracture in crystals through internal defects or sub boundaries that led to decrease in crystallite size of treated MC with respect to control.

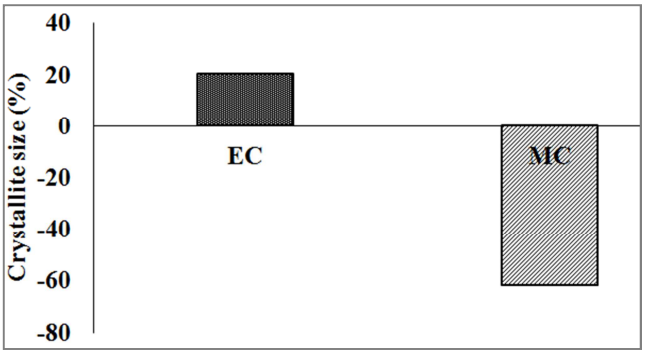

Fig. 4. *Percent change in crystallite size of treated ethyl cellulose and methyl cellulose.*

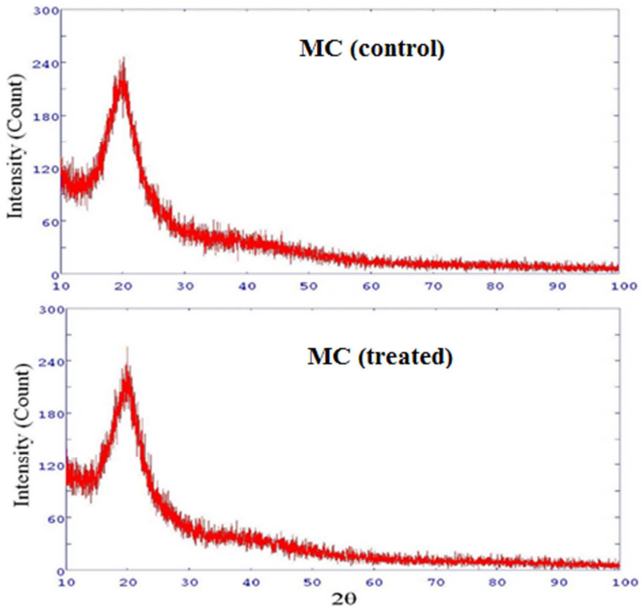

Fig. 5. *XRD diffractograms of control and treated methyl cellulose.*

3.4. Differential Scanning Calorimetry (DSC)

DSC measures the melting temperature, glass transition temperature and crystallization nature of the polymer samples. DSC thermogram of control and treated EC samples T1, T2 were illustrated in Fig. 6. DSC thermogram of control EC showed an exothermic peak at 185.13°C which was mainly due to the crystallization temperature of the sample. The second exothermic inflexion was observed on higher temperature at 334.46°C which can be attributed to thermal degradation of the control EC (Fig. 6). The treated EC (T1) also displayed similar two exothermic peak behaviour, the first peak was due to crystallization temperature (184.76°C) and the second peak at 335.24°C corresponded to thermal degradation of the treated EC. Whereas the treated EC (T2) showed exothermic crystallization peak at 185.37°C. The second exothermic was observed at 335.08°C due to decomposition of the polymer. The result showed decrease in crystallization temperature by 0.19% in EC (T1) and it was increased by 0.12% in EC (T2). This showed slight change in crystallization temperature of treated EC (T1 and T2) samples as compared to control. It is assumed here that biofield treatment has altered the internal energy of treated EC atoms, which caused change in crystallization temperature of treated EC as compared to control.

DSC thermograms of control MC and treated MC T1, T2 are presented in Fig. 7. The DSC thermogram of control and treated MC did not show crystallization peak. However, the control MC showed a broad exothermic inflexion at 301.41°C that corresponded to thermal degradation of the control. DSC thermogram of treated MC (T1) showed (Fig. 7) an exothermic transition at 301.65°C due to thermal degradation of the sample. Similarly, the treated MC (T2) sample showed slight change in thermal degradation temperature (302°C).

The enthalpy change in control and treated polymers was calculated from respective thermograms and data are presented in Table 2. The result showed that enthalpy (ΔH) of control EC was 1100 J/g whereas, the EC T1, T2 showed enthalpy value of 1020 and 841.24 J/g respectively. The percentage decrease in enthalpy for treated EC in T1 and T2 was 7.27 and 23.52% respectively as compared to control sample. However, the control MC showed a enthalpy value of 1860 J/g. After biofield treatment the enthalpy value was decreased to 1710 and 1680 J/g in treated T1 and T2 of MC, respectively. The percentage decrease in enthalpy of treated T1 and T2 of MC was 8.06 and 9.68%, respectively as compared to control. It is assumed that biofield treatment has altered the potential energy of the treated polymers that possibly led to significant change in enthalpy value as compared to control samples.

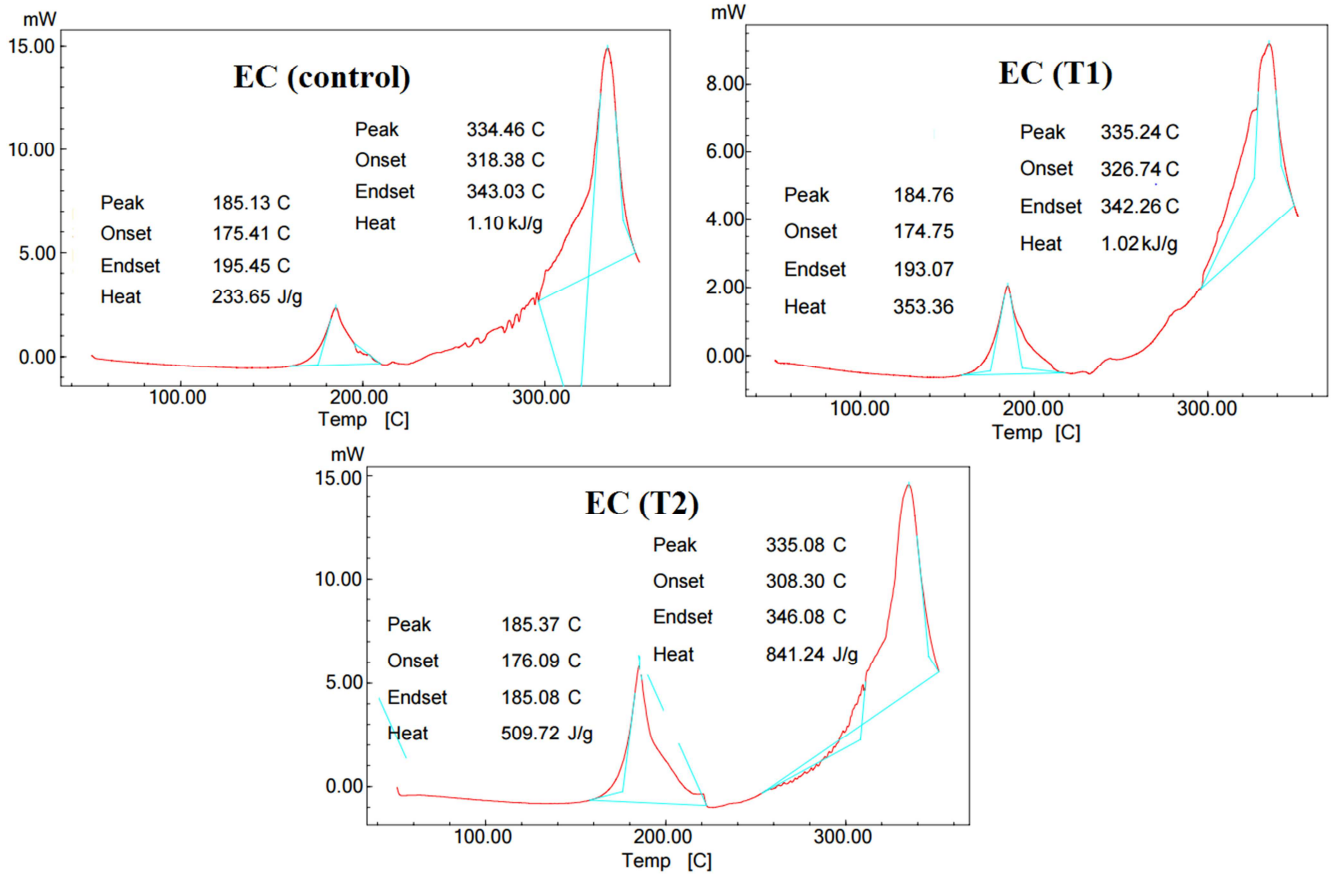

Fig. 6. *DSC thermograms of control and treated ethyl cellulose (T1 and T2).*

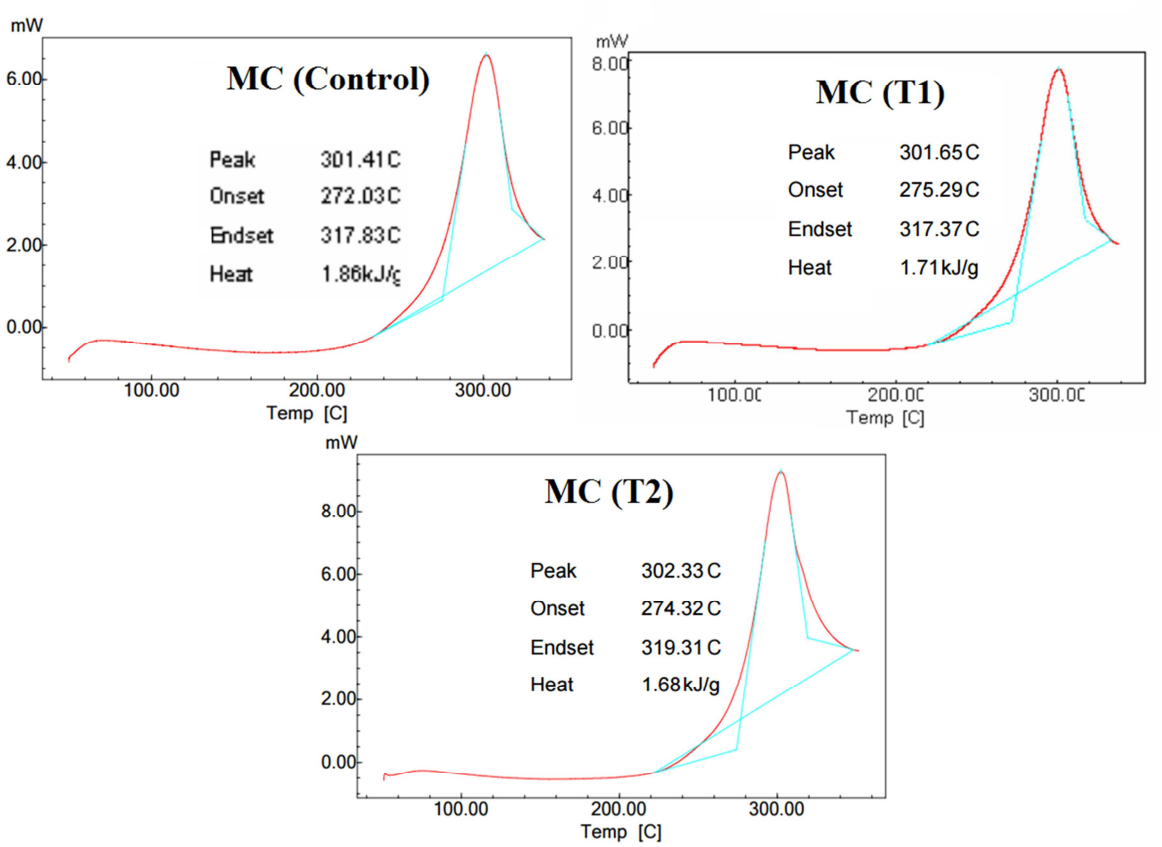

Fig. 7. *DSC thermograms control and treated methyl cellulose (T1 and T2).*

Table 2. *Enthalpy (ΔH) of control and treated polymers (ethyl cellulose and methyl cellulose).*

Sample	Ethyl cellulose		Methyl cellulose	
	ΔH		ΔH	
	Value (J/g)	% change	Value (J/g)	% change
Control	1100	-	1860	-
T1	1020	-7.27	1710	-8.06
T2	841.24	-23.52	1680	-9.68

3.5. Thermogravimetric Analysis

Thermogravimetric analysis is a tool to investigate thermal stability, oxidation, and vaporization of the polymer samples. TGA thermogram of control and treated EC samples T1, T2 are illustrated in Fig. 8. TGA thermogram of control EC sample showed one-step thermal degradation event. The sample started to degrade thermally at around 280°C and it ended at around 380°C. The EC sample lost 80.45 % of its original weight during this event. The Derivative thermogravimetry (DTG) of control EC showed maximum decomposition temperature (T_{max}) at 321°C. The thermogram of treated EC showed similar single step thermal decomposition pattern. The treated EC (T1) started to degrade at around 300°C and ended at approximately 370°C, the sample lost 57.99% of its original polymer weight. The treated EC (T1) sample showed a considerable increase in T_{max} (327°C) as compared to the control sample.

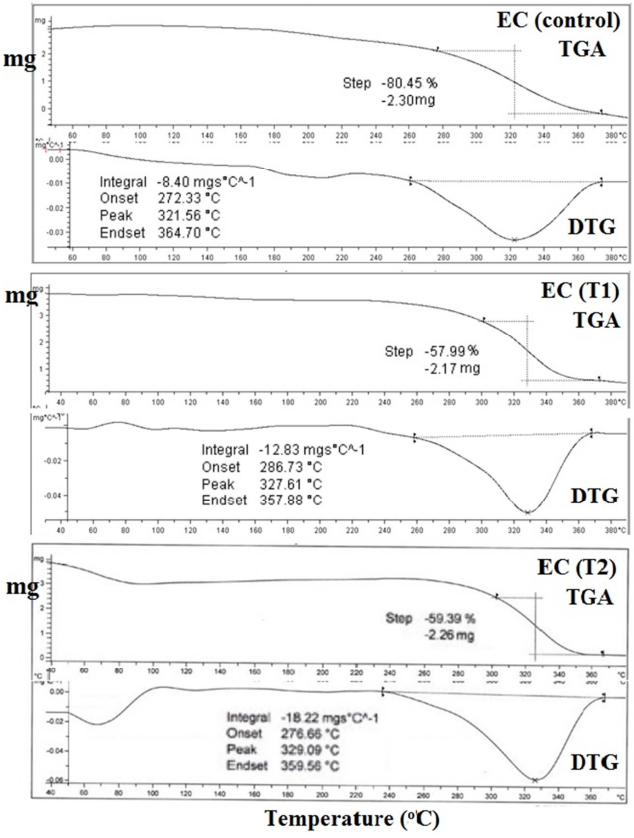

Fig. 8. *TGA thermograms of control and treated ethyl cellulose (T1 and T2).*

Whereas, the treated EC (T2) showed thermal degradation at around 302°C and degradation stopped at approximately 366°C. During this process T2 sample lost 59.39% of its weight. The DTG thermogram of treated EC (T2) showed T_{max} at 329.09°C. The comparative evaluation of the T_{max} showed increase in thermal stability of treated EC (T1 and T2) as compared to control. Szabo *et al.* showed that radiation treatment of poly (hexadecylthiophene) increases the thermal stability. They suggested that conformational changes in side alkyl chains of the polymer and crosslinking causes elevation in thermal stability [40]. Hence, it is presumed here that biofield treatment possibly caused conformational changes and crosslinking that increased the thermal stability.

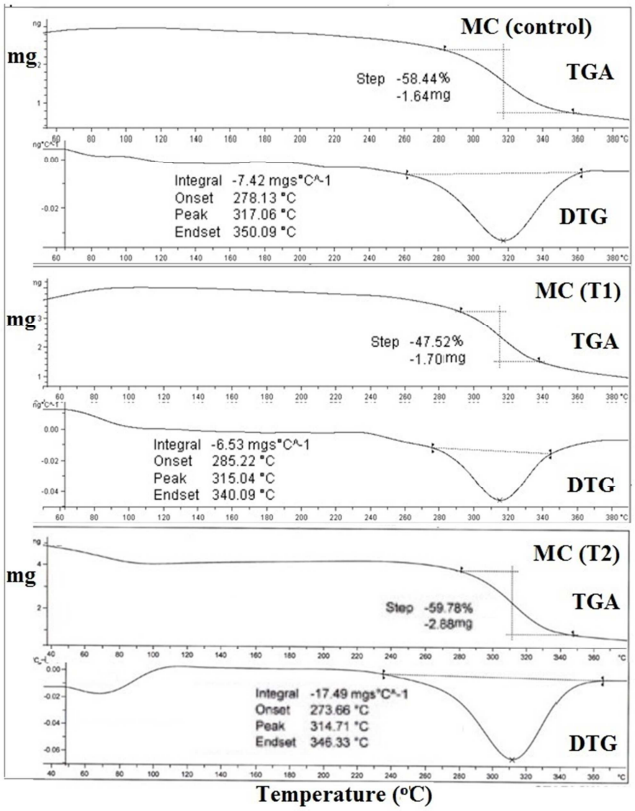

Fig. 9. *TGA thermograms of control and treated methyl cellulose (T1 and T2).*

TGA thermogram of control MC and treated MC T1 and T2 are illustrated in Fig. 9. The representative TGA thermogram of control MC showed one-step thermal degradation. The thermal degradation commenced at around 280°C and terminated at around 360°C. During this thermal process the control MC lost 59.44% of its weight. DTG thermogram of control MC showed T_{max} at 317.06°C. Whereas, the thermogram of treated MC (T1) showed similar thermal degradation mechanism. The treated MC (T1) started to thermally degrade at around 290°C and it terminated at approximately 338°C. The treated MC lost 47.52% of its weight during this process. The DTG thermogram of treated T1 MC (315°C) showed decrease in T_{max} value as compared to control sample (317.06°C). The treated MC (T2) started to degrade at around 280°C and stopped at approximately 347°C. During this process the MC (T2) lost 59.78% of its polymer weight. DTG thermogram of MC (T2) also showed decrease in T_{max} and it was observed at 314.71°C. This showed the decrease in thermal stability of MC T1 and T2 after biofield treatment. It is assumed that biofield treatment was unable to cause long range pattern in amorphous regions of MC, hence reduction in thermal stability.

4. Conclusions

The result showed significant effect of biofield treatment on physical, chemical and thermal properties of two important cellulose polymers such as EC and MC. XRD diffractogram of EC and MC (treated and control) revealed semi-crystalline nature of polymers. FT-IR spectral analysis of treated EC showed changes in C-O-C stretching with respect to control. However, the treated MC showed alteration in C-O and O-H stretching vibration peaks as compared to control. CHNSO analysis showed that biofield treatment has significantly changed the elemental composition (%H and %O) of the polymers. The treated EC showed substantial increase in crystallite size by 20.54% as compared to control. However, the treated MC showed decrease in crystallite size by 61.59% as compared to control. DSC thermogram of treated EC showed slight changes in crystallization temperature with respect to control. However, no crystallization temperature was evidenced in control and treated MC which might be due to amorphous nature of the polymer. Nevertheless, enthalpy of treated EC and MC was significantly changed after biofield treatment. TGA thermogram of treated EC showed a significant increase in T_{max} which corroborates its high thermal stability. However, the treated MC showed reduction in thermal stability as compared to control. Overall, the result suggested that biofield treatment has changed the physical and thermal properties of EC and MC. Hence, it is assumed that treated EC and MC polymers could be used for biomaterial applications.

Abbreviations

EC: Ethyl cellulose; MC: Methyl cellulose; XRD: X-ray diffraction study; TGA: Thermogravimetric analysis; DTA: Differential thermal analysis; FT-IR: Fourier transform infrared.

Acknowledgments

We thank Dr. Cheng Dong of NLSC, Institute of Physics, and Chinese academy of Sciences for permitting us to use Powder X software for analysing XRD results. The authors would like to acknowledge the Sophisticated Analytical Instrument Facility (SAIF), Nagpur for providing the instrumental facility. The authors would like to thank Trivedi Science, Trivedi Master Wellness and Trivedi Testimonials for their support during the work.

References

[1] Wintermantel E, Mayer J, Blum J, Eckert KL, Lüscher P, et al. (1996) Tissue engineering scaffolds using superstructure. Biomaterials 17: 83-91.

[2] Rambo CR, Mueller FA, Mueller L, Sieber H, Hofmann I, et al. (2006) Biomimetic apatite coating on biomorphous alumina scaffolds. Mater Sci Eng C 26: 92-99.

[3] Widmer MS, Gupta PK, Lu L, Meszlenyi RK, Evans G, et al. (1998) Manufacture of porous biodegradable polymer conduits by an extrusion process for guided tissue regeneration. Biomaterials 19: 1945-1955.

[4] Dar A, Shachar M, Leor J, Cohen S (2002) Optimization of cardiac cell seeding and distribution in 3D porous alginate scaffolds. Biotechnol Bioeng 80: 305-312.

[5] Mikos AG, Sarakinos G, Leite SM, Vacanti JP, Langer R (1993) Laminated three-dimensional biodegradable foams for use in tissue engineering. Biomaterials 14: 323-330.

[6] Powers MJ, Domansky K, Kaazempur-Mofrad MR, Kalezi A, Capitano A, et al. (2002) A microfabricated array bioreactor for perfused 3D liver culture. Biotechnol Bioeng 78: 257-269.

[7] Curtis ASG, Wilkinson CD (1998) Reactions of cells to topography. J Biomater Sci Polym Ed 9: 1313-1329.

[8] Brunette DM, Chehroudi B (1999) The effects of the surface topography of micromachined titanium substrata on cell behavior *in vitro* and *in vivo*. J Biomech Eng 121: 49-57.

[9] Langer R, Vacanti JP (1993) Tissue engineering. Science 260: 920-926.

[10] Chen D, Sun B (2000) New tissue engineering material copolymers of derivative of cellulose and lactide: their synthesis and characterization. Mat Sci Eng C 11: 57-60.

[11] Zhao K, Deng Y, Chen JC, Chen GQ (2003) Polyhydroxyalkanoate (PHA) scaffolds with good mechanical properties and biocompatibility. Biomaterials 24: 1041-1045.

[12] Madihally SV, Matthew HWT (1999) Porous chitosan scaffolds for tissue engineering. Biomaterials 20: 1133-1142.

[13] Wan YZ, Huang Y, Yuan CD, Raman S, Zhu Y, et al. (2007) Biomimetic synthesis of hydroxyapatite/bacterial cellulose nanocomposites for biomedical applications. Mat Sci Eng C 27: 855-864.

[14] Ramakrishna S, Mayer J, Wintermantel E, Leong KW (2001) Biomedical applications of polymer-composite materials: a review. Compos Sci Technol 61: 1189-1224.

[15] Muller FA, Muller L, Hofmann I, Greil P, Wenzel MM, et al. (2006) Cellulose-based scaffold materials for cartilage tissue engineering. Biomaterials 21: 3955-3963.

[16] MacNeil S (2007) Progress and opportunities for tissue-engineered skin. Nature 445: 874-880.

[17] Siro I, Plackett D (2010) Microfibrillated cellulose and new nanocomposite materials: A review. Cellulose 17: 459-494.

[18] Park JS, Park JW, Ruckenstein E (2001) Thermal and dynamic mechanical analysis of PVA/MC blend hydrogels. Polymer 42: 4271-4280.

[19] Babu VR, Kanth VR, Mukund JM, Aminabhi TM (2009) Novel Methyl Cellulose-Grafted-Acrylamide/Gelatin Microspheres for Controlled Release of Nifedipine. J Appl Polym Sci 115: 3542-3549.

[20] Mishra RK, Ramasamy K, Lim SM, Fareez IM, Majeed ABA (2014) Antimicrobial and *in vitro* wound healing properties of novel clay based bionanocomposite films. J Mater Sci Mater Med 25: 1925-1939.

[21] Prasertmanakit S, Praphairaksit N, Chiangthong W, Muangsin N (2009) Ethyl cellulose microcapsules for protecting and controlled release of folic acid. AAPS PharmSciTech 10: 1104-1112.

[22] LaFleur K, Cassady K, Doud A, Shades K, Rogin E, et al. (2013) Quadcopter control in three-dimensional space using a noninvasive motor imagery-based brain–computer interface. J Neural Eng 10: 046003.

[23] Trivedi MK, Patil S, Tallapragada RM (2013) Effect of biofield treatment on the physical and thermal characteristics of vanadium pentoxide powders. J Material Sci Eng S11: 001.

[24] Trivedi MK, Patil S, Tallapragada RM (2013) Effect of biofield treatment on the physical and thermal characteristics of silicon, tin and lead powders. J Material Sci Eng 2: 125.

[25] Trivedi MK, Patil S, Tallapragada RM (2014) Atomic, crystalline and powder characteristics of treated zirconia and silica powders. J Material Sci Eng 3: 144.

[26] Trivedi MK, Patil S, Tallapragada RMR (2015) Effect of biofield treatment on the physical and thermal characteristics of aluminium powders. Ind Eng Manag 4: 151.

[27] Trivedi MK, Patil S (2008) Impact of an external energy on *Staphylococcus epidermis* [ATCC -13518] in relation to antibiotic susceptibility and biochemical reactions - An experimental study. J Accord Integr Med 4: 230-235.

[28] Trivedi MK, Patil S (2008) Impact of an external energy on *Yersinia enterocolitica* [ATCC -23715] in relation to antibiotic susceptibility and biochemical reactions: An experimental study. Internet J Alternative Med 6: 2.

[29] Trivedi MK, Bhardwaj Y, Patil S, Shettigar H, Bulbule A (2009) Impact of an external energy on *Enterococcus faecalis* [ATCC - 51299] in relation to antibiotic susceptibility and biochemical reactions – An experimental study. J Accord Integr Med 5: 119-130.

[30] Shinde V, Sances F, Patil S, Spence A (2012) Impact of biofield treatment on growth and yield of lettuce and tomato. Aust J Basic Appl Sci 6: 100-105.

[31] Sances F, Flora E, Patil S, Spence A, Shinde V (2013) Impact of biofield treatment on ginseng and organic blueberry yield. Agrivita J Agric Sci 35: 22-29.

[32] Lenssen AW (2013) Biofield and fungicide seed treatment influences on soybean productivity, seed quality and weed community. Agricultural Journal 8: 138-143.

[33] Nayak G, Altekar N (2015) Effect of biofield treatment on plant growth and adaptation. J Environ Health Sci 1: 1-9.

[34] Patil SA, Nayak GB, Barve SS, Tembe RP, Khan RR (2012) Impact of biofield treatment on growth and anatomical characteristics of *Pogostemon cablin* (Benth.). Biotechnology 11: 154-162.

[35] Suthar V, Pratap A, Raval H (2000) Studies on poly (hydroxy alkanoates)/ (ethylcellulose) blends. Bull Mater Sci 23: 215-219.

[36] Shi P, Li Y, Zhang L (2008) Fabrication and property of chitosan film carrying ethyl cellulose microspheres. Carbohydr Polym 72: 490-499.

[37] Viera RGP, Filho GR, de Assunção RMN, da S Meireles C, Vieira JG, et al. (2007) Synthesis and characterization of methylcellulose from sugar cane bagasse cellulose. Carbohydr Polym 67: 182-189.

[38] Gaber A, Abdel-Rahim MA, Abdel-Latief AY, Abdel-Salam MN (2014) Influence of calcination temperature on the structure and porosity of nanocrystalline SnO_2 synthesized by a conventional precipitation method. Int J Electrochem Sci 9: 81-95.

[39] Raj KJA, Viswanathan B (2009) Effect of surface area, pore volume, particle size of P25 titania on the phase transformation of anatase to rutile. Indian J Chem 48A: 1378-1382.

[40] Szabo L, Cik G, Lensy J (1996) Thermal stability increase of doped poly (hexadecylthiophene) by γ-radiation. Synt Met 78: 149-153.